EXPERIMENTAL AND THEORETICAL STUDY OF A TWO PHASE HELIUM HIGH CIRCULATION LOOP

Ph. Brédy, F.-P. Juster, B. Baudouy, L. Benkheira, M. Cazanou

CEA/Saclay, DSM/DAPNIA/SACM
91191 Gif-sur-Yvette Cedex, France

ABSTRACT

In the framework of the cryogenic cooling system design of the 4T CMS magnet, heat and mass transfer has been experimentally studied at CEA-Saclay on a 9-m high helium two-phase convection loop under atmospheric pressure. The loop includes a 5-m high heated section surmounted by a 4.5-m high collector and is connected to the final CMS phase separator. The heated section of the loop is composed of seven aluminum tubes placed in parallel and heated on one side to reproduce the heating configuration of the magnet cooling system. We focused in this paper on the hydraulic characteristics of the two-phase convection loop. Evolutions of mass flow rate and vapor quality are presented and analyzed as a function of the heat flux with an equations system based on the homogeneous model.

KEYWORDS: Helium 4 normal phase, Convective heat transfer, Multiphase flows.
PACS: 67.20.+k, 44.25.+f, 47.55.Kf

INTRODUCTION

The study of hydraulic characteristics of a high two-phase normal helium (He I) circulation loop is motivated by the construction of the 4-tesla superconducting solenoid magnet for the Compact Muon Solenoid (CMS), one of the interaction detectors for the Large Hadron Collider (LHC). Designers have planned to cool this magnet with a two-phase natural circulation loop [1]. Most studies on the subject were realized in boiling two-phase forced flow configurations and few works focused on natural boiling circulation loop [2-4]. These studies were performed in a 1-m high range loop around the atmospheric pressure. Mass flow rates, pressure drops and temperature difference in the heated tube were examined. It has been shown, up to a vapor quality of 20%, that the total mass flow rate evolved with the heat flux like classical fluids [2] and that the heated tube pressure drop can be modeled with the homogeneous model with good accuracy [3]. After the realization of the 1-m high thermosiphon loop experiment, there was no getting away from carrying out a high loop recreating the same scaling than the cooling circuit of CMS. The main goals are to reach the same thermal and hydraulic conditions as in the magnet and to explore a larger range than the nominal heat load in considering the possibility of having a height of several meters between the phase separator and the lower part of the cooling loop and several circuits in parallel with the specific hydraulic singularities of the final loop.

EXPERIMENTAL APPARATUS

The CMS superconducting magnet consists of 5 independent modules, each of them being cooled by 2 sets of circuits (square aluminum heat exchangers welded on the magnet cylinder) [5]. Thermal loads are estimated to be around 50 and 100 W per module (25 and 50 W per circuit) corresponding respectively to the static and the slow discharge conditions. It was decided to recreate the most unfavorable thermal case which appears on the central module only equipped with seven cooling pipes. Our experimental facility at Saclay, a 8-m deep and 0.88-m diameter cryostat, did not allow us to keep all the module geometrical characteristics, in particular, the curve of the magnet cylinder (R=3.473 m) and the total hydrostatic head (11.68 m). Consequently, we kept all the diameters (0.014-m heated tube inner diameter, inlet and outlet lines and their main singularities) and the manifolds geometry used for the seven branches. But we used 5-m long straight heated branches (6.95 m on CMS) and a 4.56-m high adiabatic upward line (5.07 m on CMS). Therefore, downward and upward hydrostatic heads are respectively 9.22 m and 9.57 m for our loop whereas they are 11.68 m and 12.03 m in the CMS final design.

Having the CMS phase separator cryostat at our disposal after its cryogenic acceptance tests at Saclay, we built a test facility using this horizontal equipment and our vertical cryostat. General characteristics of the loop are given in FIGURE 1. The overall height of the all loop equals 9.60 m.

To perform all the measurements, we used the phase separator cryostat dedicated equipment (pre-cooling valves and circuits, pressure, liquid level and temperature sensors, return liquid flow-metering based on the overflowing method) and we added specific instrumentation for the vertical loop including:

-a low pressure drop liquid helium Venturi flow-meter located on the adiabatic downstream line. We used the classical theoretical law with a discharge coefficient of 0.97.

- 91 heating elements on the seven vertical branches (MINCO thermofoil).

Other instrumentation were also installed such as temperature sensors distributed along the circuits, differential pressure gauges on each heated branch , differential pressure gauges between phase separator and the lower point of the loop and mass-flow measurements on the gas outlets of the system. The results and analysis of these measurements will be presented and discussed elsewhere.

All data were stored at a speed of 1 Hz. The LHe tank of the horizontal cryostat (800 l total volume) was initially filled at 50% of the level gauge before each measurement campaign (1% corresponding to 7.4 mm high) and the pressure of the phase separator was regulated around 1.25 bars absolute (with some instabilities due to the large size of the valve designed for final boil-off of the CMS magnet).

EXPERIMENTAL RESULTS AND DATA REDUCTION

Since a lot of measurements have been made during the experimental sessions, we chose to present here the measurements carried out with identical heating power in each of the seven pipes. The range investigated for the total power electrically deposited (Q) in the heaters goes from 10 to 405 watts.

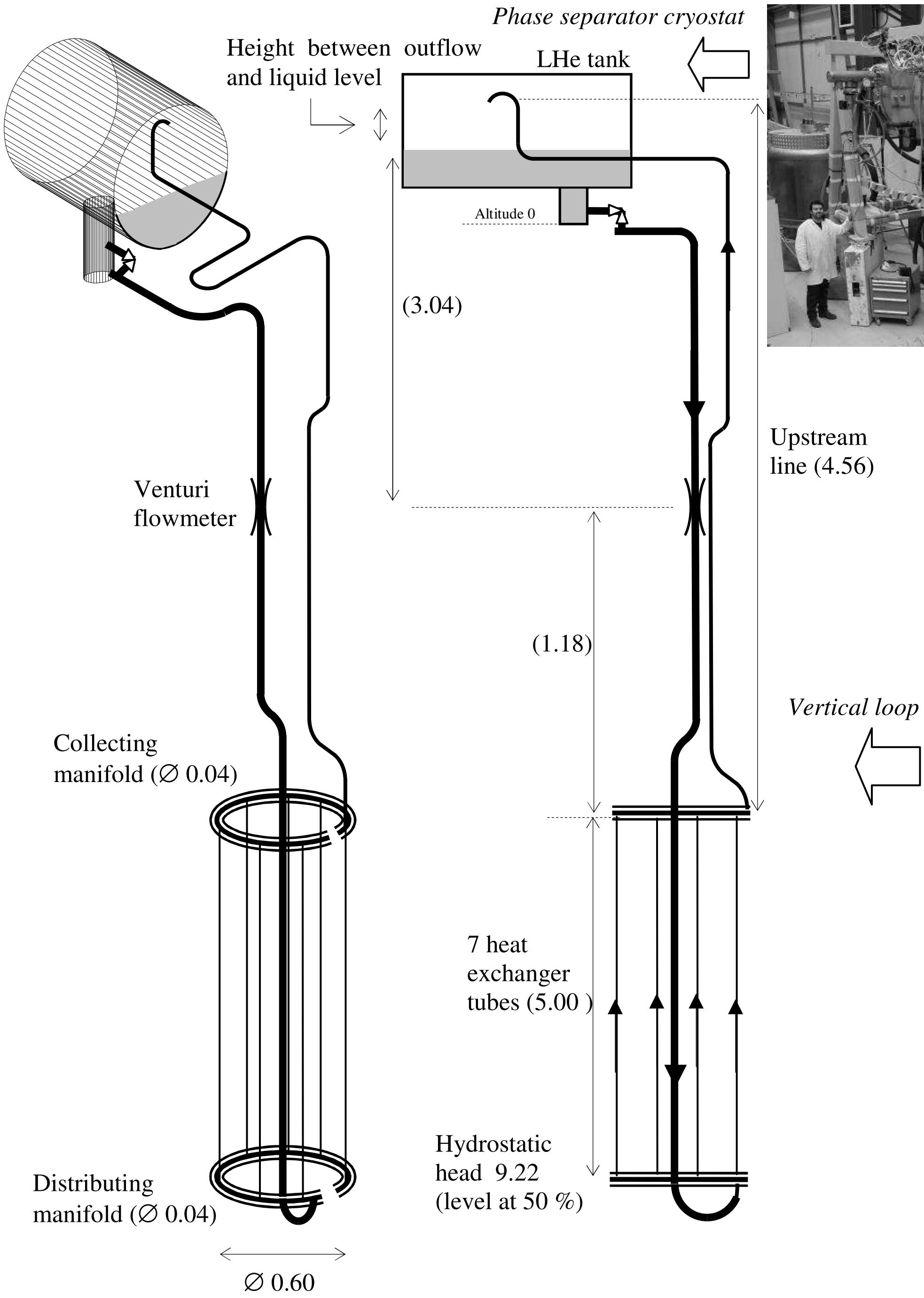

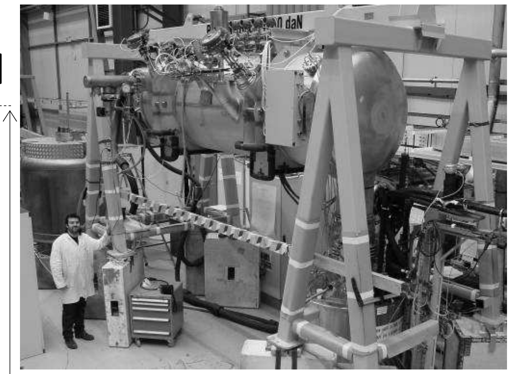
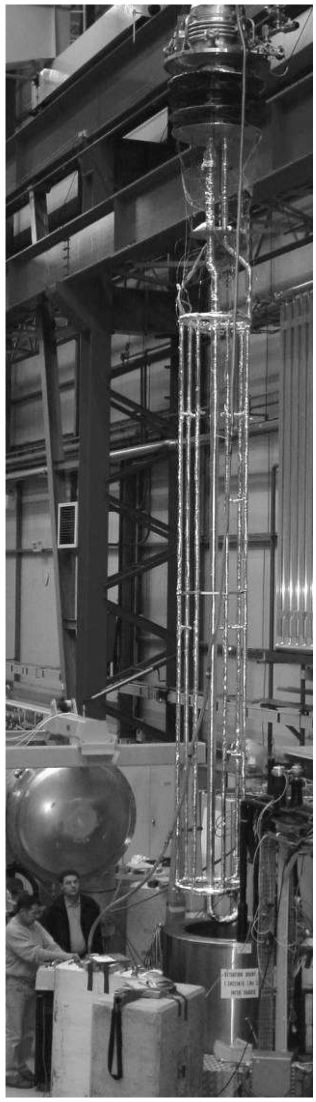

FIGURE 1. Schematics views and pictures of the main parts of the test loop

TABLE 1. Summary of the loop's geometrical characteristics

Sectors	**Dimensions (m)**	**Associated equipment**
On/Off cryogenic valve	DN 80 Cv = 215	
Adiabatic downward line	h=9.15 × ∅ 0.057	Venturi flowmeter (inlet ∅ 57.1 neck ∅ 22)
7 heat exchanger tubes	h=5.00 × ∅ 0.014	7 × 13 Heating elements (7x 177 Ω)
Adiabatic upward line	h=4.56 × ∅ 0.041	
Height between outflow and liquid level (50% level)	h=0.35	Overflowing flowmeter (outlet liquid)

Operating Mode

All the heating resistors of each pipe are connected in series and we impose a constant and measured current in the circuit. For a given current, a typical 10-minute-long acquisition is made. At fixed current, the mass flow is measured and averaged over this period. Each time we change the current, we observe a transient regime in the measured flow. The corresponding period is excluded from the above mentioned average.

An experimental session begins when the liquid level in the phase separator equals 50% and ends when this level decreased down to 35%. We will see further that this point has a significant influence on the total mass flow especially for low power values.

The vapor quality is currently computed from the following conservation equation:

$$G.\Delta\left(H+\frac{v^2}{2}+gz\right)=Q \leftrightarrow G.\left(x.L_v+\Delta\frac{v^2}{2}+gh\right)=Q \qquad (1)$$

G is the total mass glow, x is the vapor quality, L_v is the latent heat estimated at the phase separator pressure (1.25 bars, L_v=19200 J/kg), h is the height between the liquid level in the separator and the outflow point of the exhaust pipe, v is the velocity of the flow. Computations show that the kinetic energy term is completely negligible in the investigated mass flow range.

Data reduction

The estimated uncertainties on the electrical measurements are taken equal to 1%.

The cryostat static heat loads were measured and lead to an enhancement of the effective deposited power. We estimated that the net power which has to be added to the injected electrical power is comprised between 0 and 2 watts. We therefore systematically add 1 watt to the injected power and 1 watt to the error bar on power measurements.

The error bar on the mass flow measurements takes into account the uncertainties on pressure difference measurements on the Venturi flow meter, the fluctuations (standard deviation) of the measured mass flow over the considered acquisition period and a supposed 1% systematic error due to the discharge coefficient. This leads to error bars going from 2% (high Q values) to 25% at 10 watts.

The error bar on the computed quality x is deduced from the error bars on Q and G.

Results

As the FIGURES 2 and 3 show, the maximum measured mass flow equals 165 g/s leading to a computed vapour quality of 13% corresponding to a maximum liquid Reynolds number (exhaust pipe) of 1.7 10^6. The vapour quality does not tend to 0 with Q but seems to tend to a value comprised between 2 and 3%. This results from the fact that, whatever may be the liquid level in the phase separator, the outflow of the two-phase helium systematically occurs above that liquid level (see FIGURES 1). As a consequence, for very low power values, the friction in the loop becomes negligible and the difference between the hydrostatic heads (ρgh) of the downward and upward branches tends to 0. Seeing that the height (h) of those branches are not equal, necessarily the average fluid densities are different in the two branches and a minimum vapour quality must be created to start a permanent thermosiphon regime.

THEORITICAL RESULTS

Assumptions of the model

Our model is based on the homogeneous assumption widely described elsewhere [6, 7]. Let us just remind that the two phases are supposed to flow with the same velocity *v*. The governing equations (Continuity, Momentum and Energy) are:

$$G = \rho A v \tag{2}$$

$$\frac{G}{A}\frac{dv}{dz} = -\frac{dp}{dz} - \left(\frac{dp}{dz}\right)_f - \rho g \cos(\theta) \tag{3}$$

$$\frac{dq}{dz} = G\frac{d}{dz}\left(H + \frac{v^2}{2} + gz\cos(\theta)\right) \tag{4}$$

ρ is the mean density of the liquid-vapor mixture, A is the cross-sectional area, H is the mean enthalpy of the mixture, θ is the angle between the element dz (curvilinear abscissa) with a vertical line, dp_f is the elementary friction pressure drop, dq is the elementary power deposited in dz. In our code, we consider the classical two-phase friction correlation:

$$\left(\frac{dp}{dz}\right)_f = \phi_{fo}^2 \frac{f}{D_h}\frac{1}{2}\frac{G^2}{\rho_l A^2} \tag{5}$$

$$f = \frac{0.3164}{\mathrm{Re}_l^{0.25}} \tag{6}$$

ϕ^2_{f0} is the two-phase frictional multiplier [6], the kinetic term in Equation (5) and the Reynolds number in Equation (6) are evaluated considering the total flow as liquid. D_h is the hydraulic diameter of the considered element dz.

In addition to those classical assumptions, the main characteristics of our code are:

- All the singularities of the loop (valves, Venturi flow meter, section changes, flow separations and junctions, elbows, exhaust) are taken into account. The singular pressure drops are treated like the friction pressure drops using the two-phase frictional multiplier. All our correlations are taken from [8].
- The loop is discretized in small element (typically $dz \approx 5$ cm) where the governing equations are solved.
- The fluid properties are renewed in each element but the viscosities.
- The sub-cooled single-phase part of the loop is studied.
- In the multi-branches part of the loop, all the pressure drops are computed assuming that the mass flows are identical in all branches and just the middle tube is considered.
- We use an iterative method where, for an imposed deposited power, we adapt the total mass flow so that the outflow computed pressure equals the separator pressure.

Theoretical results

The computed vapour quality and mass flow values are plotted on FIGURES 2 and 3. First of all, one may state a very satisfactory agreement between theoretical and experimental results especially below 250 watts ($x \approx 8\%$, $G \approx 150$ g/s). We chose to present in Table 2 the detailed results for a 50% and 35% liquid level in the phase separator.

As expected, the total pressure drop essentially comes from the upward part of the loop: in the investigated range, the downward part only contributes to 15-20% of the total pressure drop. Moreover, this contribution is dominated by the pressure drop in the Venturi flow meter. This pressure drop has been measured and is equal to 20% of the measured pressure difference between the inlet and the neck of the Venturi flow meter.

The total pressure drop is dominated by the singularities especially at the inlet and outlet of the heated tube which contribute to about 30% of the total singularities pressure drop. The total pressure drop in the heated tubes represents more or less the half of the total pressure drop, the friction pressure drop in those tubes represents one third.

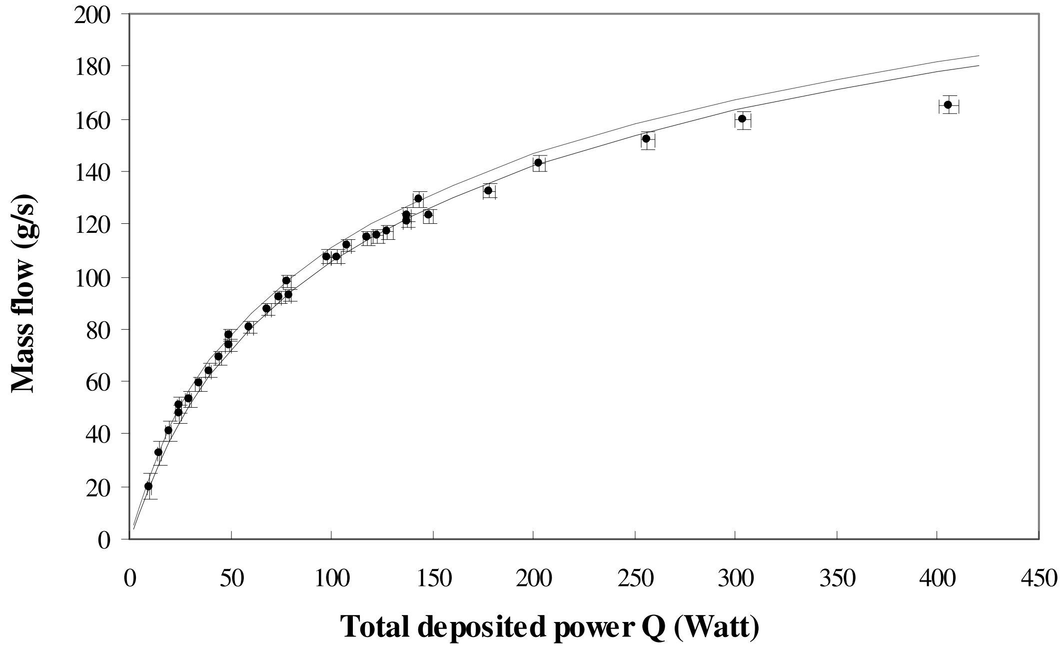

FIGURE 2. Mass flow as a function of the total deposited power. Plain lines are theoretical curves for a 50% liquid level (upper curve) and a 35% liquid level.

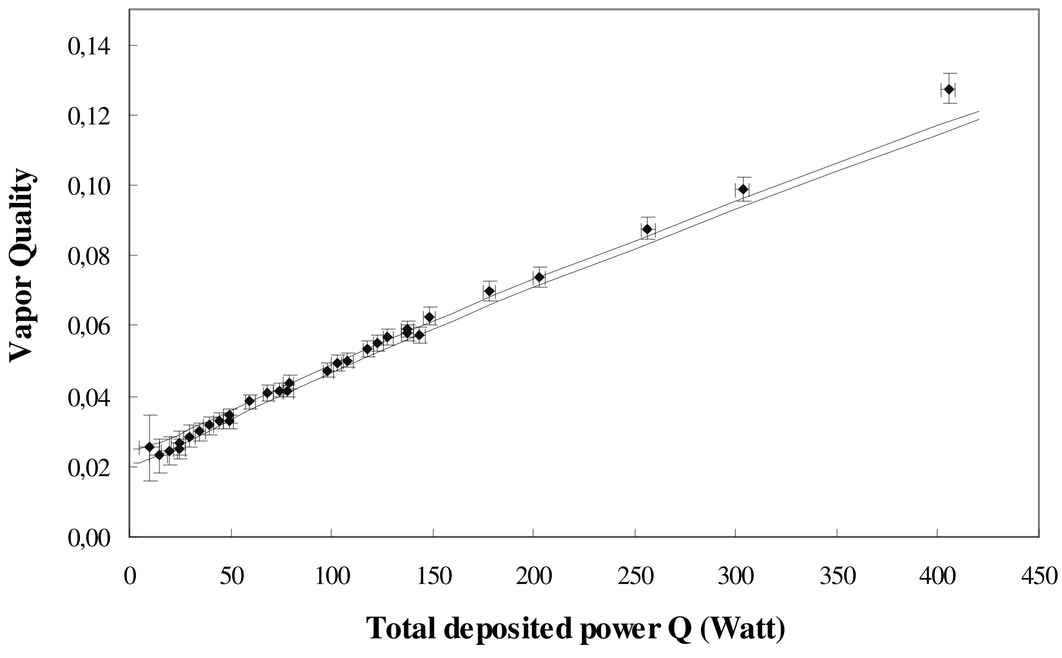

FIGURE 3. Vapor quality as a function of the total deposited power. Plain lines: theoretical curves for a 35% liquid level (upper curve) and a 50% liquid level.

TABLE 2. Details of the theoretical results

Deposited Power (watt)	25	50	100	200	300	25	50	100
Phase separator liquid level (%)	50	50	50	50	50	35	35	35
Mass Flow (g/s)	50.0	77.9	111	147	167	44.2	72.1	106
Outlet Vapor Quality (%)	2.6	3.3	4.7	7.1	9.3	2.9	3.6	4.9
Total loop pressure drop (friction+sing.) (mbars)	1.53	3.63	7.34	13.2	17.8	1.22	3.14	6.71
Total downward pressure drop (mbars)	0.22	0.52	1.04	1.80	2.33	0.17	0.44	0.94
Venturi flow meter pressure drop (mbars)	0.14	0.34	0.69	1.21	1.58	0.10	0.29	0.63
Total upward pressure drop (mbars)	1.32	3.11	6.30	11.4	15.4	1.05	2.70	5.77
Total friction pressure drop (mbars)	0.75	1.70	3.30	5.72	7.58	0.61	1.49	3.03
Total singular pressure drop (mbars)	0.78	1.93	4.04	7.45	10.2	0.61	1.66	3.68
Pressure drop (friction + sing.) in tube (mbars)	0.77	1.79	3.56	6.27	8.37	0.61	1.55	3.25
Single-phase part length in Tube (mbars)	3.30	2.80	2.15	1.55	1.25	3.05	2.65	2.05
Equation (1) enthalpy term (G.x.Lv)	24.8	49.7	99.6	199	299	24.8	49.7	99.5
Equation (1) gravitational term (G.g.h)	0.19	0.28	0.40	0.53	0.60	0.21	0.34	0.49
Equation (1) kinetic term ($G.\Delta v^2/2$)	$8 10^{-4}$	$4 10^{-3}$	0.02	0.07	0.14	$5 10^{-4}$	10^{-3}	0.02

The computations confirm that the vapour quality does not tend to 0 with Q. We found that its limit values are 2.1 and 2.5% for 50 and 35% separator liquid level respectively. Correlatively, the computed ratio of the mass flows corresponding to those different levels tend to 1.21 (Equation (1)). The level difference (15% ↔11.05 cm) between the two cases induces a constant hydrostatic head difference (1.3 mbars) and so a constant contribution to the driving term of the circulation in the loop. As Q increases, and so G, the driving term, which must balance the friction in the loop, increases and the added value due to higher level becomes negligible: the mass flows ratio tends to 1.

As previously said, the kinetic energy term is negligible in Equation (1). Moreover computations carried out neglecting the acceleration term of Equation (3) (left side term) shows no significantly different results: a few percents mass flow enhancement at 300 W and a few thousandths of percent at 50 W.

We remark that, in the working range of CMS, more than the half of the heated tube is cooled by single-phase helium. This is directly linked to the relatively low measured and computed x-values in that range: for a given energy Q, a low vapour quality value leads to high mass flow value and as a consequence to large single-phase functioning regime.

As Q increases, even if the discrepancy does not exceed 10% for the maximum measured Q-values, the model tends to compute lower values than those measured beyond 250 watts. We may propose some explanations to this:

- The assumption of equal mass flows in each branch is valid only when branches are hydraulically decoupled, in other words when pressure drop effects in the distributing and collecting manifolds are negligible, which is correct at low mass flows.
- The validity range of some correlations used for singular pressure drop (especially in case of flow bifurcations) is not explicitly specified by the authors. We have no guaranty, at present, that they are applicable at high Reynolds number. This point is under investigation.

Extrapolation to CMS Magnet

We have adapted the code to CMS geometry. The 25-watt nominal heat load leads to computed mass flows of 44 and 49 g/s for the separator liquid levels of 35 or 50% respectively, corresponding vapour qualities are 2.9 and 2.6%.The 50-watt slow discharge regime heat load leads to computed mass flows of 71 and 75 g/s, corresponding vapour qualities are 3.7 and 3.4%.

As expected, the vapour quality values are higher than for the experimental loop, but very slightly. It must be remarked that, as previously said, the friction in the heated tube of the experimental loop represents about only one third of the total pressure drop. CMS geometry mainly differs by a factor 2 increase in heated tube length. As a consequence (at 50 watts and 50% level) the total pressure drop goes from 3.63 mbars (*cf.* TABLE 2) to 4.92 mbars. That 1.3 mbar difference represents only 1% of the downward hydrostatic head, it is balanced by a 1% decrease of the upward mean fluid density, which is obtained by a 3% increase of the vapour quality and so an identical mass flow decrease. And finally it is important to remark that the extrapolation is made in the region where the code correctly reproduces the experimental values.

CONCLUSION

As a 10% vapour quality limit value is generally admitted for a safe thermosiphon loop functioning, we therefore have the advantage of a comfortable margin as both measurements and computations leads to vapour quality values lower than 4% in the expected nominal thermal conditions of CMS magnet. The next steps related to the thermosiphon hydraulics study are of two kinds:

- Improving the code, especially to allow different mass flows in each branch. On one hand, we can expect a better fit of the experimental data particularly for high mass flows, on the other hand and above all, that improved tool will allow the analysis of the data obtained with asymmetric heating on branches.
- Analysing all the other obtained experimental results likely to valid the code, particularly the pressure measurements.

The heat transfer analysis is to be done. Preliminary results are encouraging as they show heat transfer coefficients of 1500-2000 $W/m^2.K$, higher than the design values.

ACKNOWLEDGEMENTS

The authors would like to warmly thank Drs. F. Kircher, A. Hervé and D. Campi for their continuous and friendly support and to J.C. Toussaint for technical assistance. This work was supported by the CERN-CEA collaboration for the 4T CMS magnet construction.

REFERENCES

1. Lottin, J. C. and Juster, F.-P., "Liquid Helium Thermosiphon for the 4 Tesla CMS Solenoid," in Advances in Cryogenic Engineering 43, edited by P. Kittel, Plenum Press, 1998, pp. 1505-1511.
2. Baudouy, B., "Heat and mass transfer in two-phase He I thermosiphon flow," in Advances in Cryogenic Engineering. 47 B, edited by S. Breon, AIP, 2001, pp. 1514-1521.
3. Baudouy, B., "Pressure drop in two-phase He I natural circulation loop at low vapor quality," in International Cryogenic Engineering Conference proceedings 19, edited by P. S. G. Gistau Baguer, 2002, pp. 817-820.
4. Baudouy, B., "Heat transfer near critical condition in two-phase He I thermosiphon flow at low vapor quality," in Advances in Cryogenic Engineering 49, edited by S. Breon, AIP, 2003, pp. 1107-1114.
5. Hervé, A., "Status of the construction of the CMS magnet," in IEEE Transactions on Applied Superconductivity 14, n°2, edited by I. S. Council, 2004, pp. 542-547.
6. Collier, J. G., Convective boiling and condensation, McGraw-Hill, London, 1972.
7. Wallis, G. B., One-dimensional Two-phase flow, MacGraw-Hill, New York, 1969.
8. Idel'Cik, I. E., Mémento des pertes de charge, Eyrolles, 1986.